Bottom trawling – in a flume tank

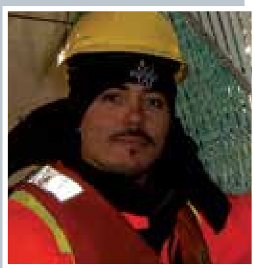

Tomas Araya-Schmidt

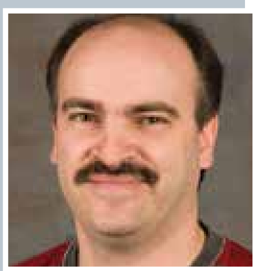

George Legge

Mark Santos

Researchers Araya-Schmidt, Legge, Santos, Bayse, and Winger present a novel technique for comparing footgears using models and simulated seabed conditions in a flume tank.

Who should read this paper?

This paper should be read by fishing gear technologists interested in innovative solutions to address seabed impact, as well as scientists and the general public interested in environmental impacts reduction and improving sustainability of fisheries.

Why is it important?

The paper presents an innovative method to estimate drag and seabed contact reduction of a new footgear technology using a flume tank and bottom trawl engineering models. Footgears were assessed during simulated smooth, semi-rough, and rough seabed conditions. To the authors' knowledge, using simulated seabed in a flume tank has never been done before in this field. The footgear under development and presented in this study is unique in its type and could represent a significant advancement in footgear technology; it may encourage other fishing gear technologists and industry to develop and test new solutions to reduce environmental impacts and improve efficiency of bottom trawl fisheries.

Sea trials are planned to fully develop and test the aligned-rolling footgear during the summer/fall of 2021. If sea trials are proven to be successful, this technology has a high probability of being implemented, contributing to reduce seabed impact in the Canadian Northern shrimp fishery and other bottom trawl fisheries. Based on the outcome of the sea trials, the authors expect that the technology will be ready for implementation in 2022.

About the authors

Mr. Tomas Araya-Schmidt is a PhD candidate working on fishing gear technology at the Centre for Sustainable Aquatic Resources, located at the Fisheries and Marine Institute, Memorial University. He holds a B.Sc. in fisheries engineering from the Pontificia Universidad Católica de Valparaíso in Chile, and an M.Sc. in environmental science from Memorial University.

Mr. George Legge is the Facility Supervisor with the Centre for Sustainable Aquatic Resources, located at the Fisheries and Marine Institute, Memorial University. Mr. Legge has over 30 years of experience in the operation of the flume tank as well as the scaling, construction, and evaluation of model fishing gear. He holds a Diploma in Mechanical Engineering Technology and a 3rd Class Certificate in Power Engineering.

Mr. Mark Santos is the Fishing Gear Technologist of the Centre for Sustainable Aquatic Resources at the Fisheries and Marine Institute of Memorial University. He has over 10 years' experience in applied fisheries research. He holds a B.Sc. from NSAC/Dalhousie University and a Master's of Technology Management degree from Memorial University.

Dr. Shannon Bayse is a Research Scientist at the Centre for Sustainable Aquatic Resources, located at the Fisheries and Marine Institute, Memorial University. He holds a B.Sc. from Virginia Tech, an M.Sc. from Nova Southeastern University, and a PhD from the University of Massachusetts. Dr. Bayse is an accomplished scientist, publishing several peer-reviewed manuscripts on fish capture, trawl technology, and fish physiology.

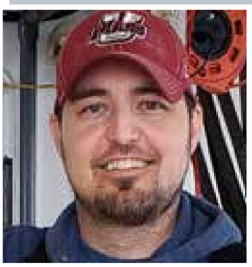

Dr. Shannon Bayse

Dr. Paul Winger is the Director of the Centre for Sustainable Aquatic Resources, located at the Fisheries and Marine Institute, Memorial University. He holds a B.Sc. in marine biology and oceanography from Dalhousie University, as well as an M.Sc. in biopsychology and a PhD in cognitive and behavioural ecology, both in the field of fish capture, from Memorial University. Dr. Winger has a broad knowledge of fisheries issues with extensive experience in the area of fishing gear innovation.

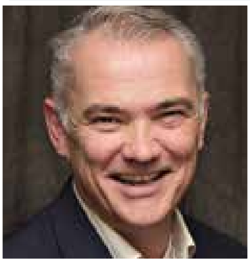

Dr. Paul Winger

FLUME TANK TESTING OF AN INNOVATIVE FOOTGEAR TECHNOLOGY USING SIMULATED SEABEDS

T. Araya-Schmidt, G. Legge, M. Santos, S.M. Bayse, and P.D. Winger

Centre for Sustainable Aquatic Resources, Fisheries and Marine Institute, Memorial University of Newfoundland, St. John's, N.L., Canada

ABSTRACT

There have been many advancements in bottom trawls to reduce physical and biological impacts on benthic habitats. In this study, an innovative aligned-rolling footgear was designed and evaluated for use in the Northern shrimp (*Pandalus borealis*) fishery in Eastern Canada. We document a novel technique for comparing traditional and experimental footgears using engineering models and simulated seabed conditions in a flume tank. Footgears were compared using direct observation and by measuring warp load during simulated smooth, semi-rough, and rough seabed conditions in contact with bosom or wing footgear sections. Results revealed that the traditional footgear bottom trawl experienced significantly higher warp loads for smooth (0.26 t higher), semi-rough (0.68 t higher), and rough seabed conditions (0.74 t higher) in the bosom section. In the wing section, traditional bottom trawl produced significantly higher warp loads for smooth (0.38 t higher) and rough seabed conditions (0.30 t higher). Bottom trawl with aligned-rolling footgear reduces seabed contact up to 71.5% depending upon depth of penetration modelled. To our knowledge, this study represents the first attempt at using simulated seabed conditions in a flume tank testing footgear technology.

KEYWORDS

Aligned-rolling footgear; Seabed impact; Bottom trawling; Flume tank

INTRODUCTION

Since the 1950s, bottom trawls have been widely used to target demersal species in an efficient and economically viable manner [Valdemarsen, 2001; Watson et al., 2006; Valdemarsen et al., 2007]. Bottom trawls account for almost one-quarter of the total wild marine landings annually [Amoroso et al., 2018], which represents a substantial contribution to global food security [Kaiser et al., 2016]. However, these bottom-contacting fishing gears can result in physical and biological impacts on benthic habitats [Hiddink et al., 2017; Sciberras et al., 2018].

Bottom trawls typically employ heavy components to move, herd, guide, and finally capture demersal fish and shellfish in fishing gear [Montgomerie, 2015]. The extent of contact and seafloor penetration varies with the trawling operation, which are customized for the target species, depth, and seabed type [Løkkeborg, 2005; He, 2007; Sciberras et al., 2018; Depestele et al., 2019]. Bottom trawls can cause adverse effects on benthic species and habitat. Direct effects include mortality of benthic organisms [Collie et al., 2005], alteration to seafloor composition and bathymetry [Depestele et al., 2019], reduction of topographic complexity [O'Neill and Ivanović, 2016], and changes to sediment biogeochemistry [Mayer et al., 1991; Sciberras et al., 2016]. In the first few days after trawling, direct mortality and bycatch discarded from fishing vessels can attract scavengers to the trawled area [Collie et al., 2017]. In the long term, persistent trawling of an area can reduce benthic biomass, diversity, and numbers of individuals, which in turn can reduce productivity, change trophic structure and function of the benthic community, as well as generate changes to body size and age structure of benthic organisms [Jennings et al., 2001; Hiddink et al., 2006]. Ultimately, chronic trawling can produce a change towards communities dominated by species with faster life histories [Tillin et al., 2006; Johnson et al., 2015; Van Denderen et al., 2015].

Growing concerns about seabed impacts [Kaiser et al., 2016] have led to the study of new technologies to reduce the area of contact, weight, or penetration depth of fishing gear components on the seabed, as well as the reduction of bycatch of benthic species [He, 2007; He and Winger, 2010]. Much of this innovation has focused on improving the footgear of bottom trawls and has led to the development of footgears that roll over the seabed [Ball et al., 2003; He and Balzano, 2010], or that are aligned with the towing direction [Winger et al., 2018], or have reduced area/points of contact [Nguyen et al., 2015a; Brinkhof et al., 2017; Larsen et al., 2018].

Roller footgear is currently used by offshore trawlers targeting Northern shrimp (*Pandalus borealis*) in Eastern Canada. Large rubber discs are threaded onto the footgear chain with rubber and steel spacers (i.e., lancasters) between them. The footgear is constructed in large sections that are connected together using swivels. The footgear is called "roller footgear" because these large sections are free to roll, allowing the footgear to move over hard rocky seabed and protect the trawl from damage [Montgomerie, 2015]. However, recent findings during fishing operations have shown that the footgear sections are rolling at extremely low rates [Araya-Schmidt et al., 2021], which may produce higher sliding, digging, and drag forces [Fridman, 1986; Esmaeili and Ivanović, 2014; Winger et al., 2018].

Footgear components with no, or limited, rotation and a larger contact area with the seabed likely cause increased damage to benthic structures, higher mortality and exposure of benthic species, as well as increased sediment remobilization [O'Neill and Summerbell, 2016; Hiddink et al., 2017; Depestele et al., 2019]. Aligned footgears reduce seabed contact by "aligning" footgear discs in the direction of the tow. In the 1940s, the first known aligned wheel footgear was designed in Germany. Presumably, footgears that can roll over the seabed were originally designed to reduce fuel consumption [He and Balzano, 2010]. However, it has been shown that aligned footgear designs can reduce substrate material in the trawl net, bycatch, drag, area of contact, and presumably, seabed impacts [Ball et al., 2003; Zachariassen, 2004; He and Balzano, 2010; Winger et al., 2018].

A critical component of the fishing gear development cycle is flume tank testing of engineering models [Winger et al., 2006]. This allows fishing gear technologists to identify design defects, measure changes to trawl geometry due to different riggings or towing speeds, measure forces, and document the dynamic motions of the fishing gear. Several footgear technologies have been tested in flume tanks [Ball et al., 2003; Grimaldo et al., 2014; Nguyen et al., 2015a; Winger et al., 2018]. Laboratory experiments have been used to study the impacts of trawl doors on the seabed and infaunal bivalves [Gilkinson et al., 1998]. Seabed penetration experiments for beam trawls have been performed in towing channels [Paschen et al., 2002]. In recent years, numerical modelling of ground gear elements has been developed to estimate contact forces [Ivanović et al., 2008], penetration depth [Ivanović et al., 2011; Ivanović and O'Neill, 2015], soil displacement [O'Neill and Ivanović, 2016], and drag force [Ivanovic et al., 2009]. To our knowledge, testing model trawls with new footgear technologies is usually conducted in flume tanks with a flat moving seafloor. While a moving seafloor is better than no moving seafloor, the lack of texture does not allow fishing gear technologists to make inferences on the performance of the footgear over coarser seabeds.

Building on previous roller footgear concepts [Ball et al., 2003; Zachariassen, 2004; He and Balzano, 2010; Winger et al., 2018], this study designed and evaluated an innovative aligned-rolling footgear. We document a novel technique for comparing traditional and experimental footgears using engineering models and simulated seabed conditions in a flume tank. Footgears were qualitatively compared using direct observation and quantitatively assessed by measuring warp load during smooth, semi-rough, and rough seabed conditions in contact with bosom and wing footgear sections. The results are discussed in relation to expected seabed impact, prototype validation, and previous footgear innovations.

METHODS

Modelling of Bottom Trawl

A linear model scale of 1:10 was selected in

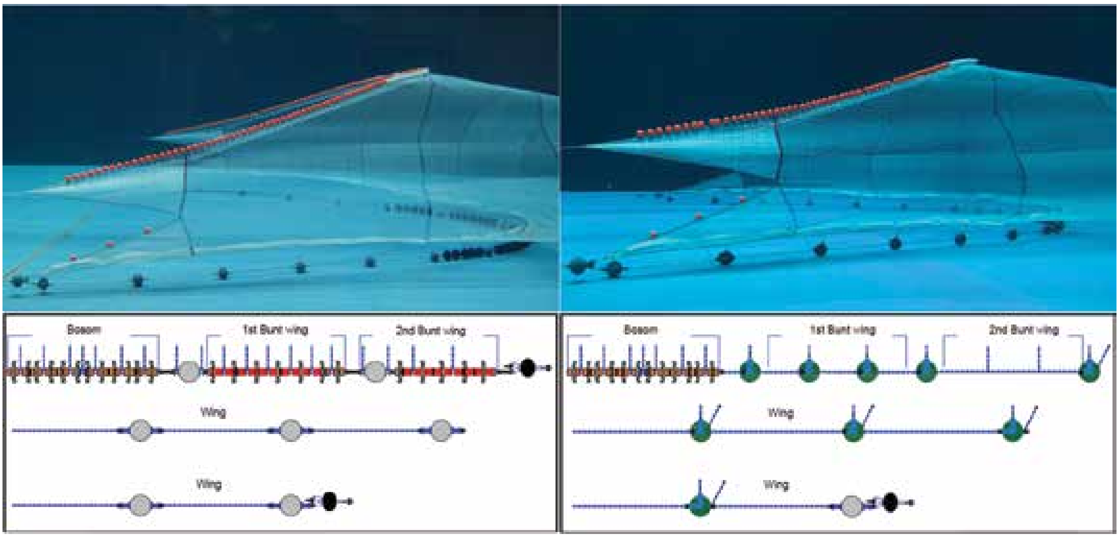

Figure 1: Traditional (left) and aligned-rolling (right) footgears. Bosom section and one side of bunt wing and wing sections are shown for the footgears. Aligned-rolling wheels are shown in green.

order for the bottom trawl to fit in the flume tank and achieve the desired wingspread commonly used by the commercial fishing vessels (approximately 37 m). The model was constructed at the Fisheries and Marine Institute's Centre for Sustainable Aquatic Resources using Froude scaling laws [Tauti, 1934; Fridman, 1973; Hu et al., 2001]. Force, geometric, kinematic, and dynamic modelling laws are commonly used in model scaling to approximate full-scale bottom trawl characteristics [Fiorentini et al., 2004; Queirolo et al., 2009; Sala et al., 2009; Nguyen et al., 2015b; Thierry et al., 2020]. The fundamental modelling laws can be summarized as follows, where *f* and *m* in the subscripts represent the full-scale and model, respectively:

$$\lambda = L_f / L_m \qquad (1)$$

$$A_m = A_f / \lambda^2 \qquad (2)$$

$$F_m = (F_f / \lambda^3)(\rho_m / \rho_f) \qquad (3)$$

$$\lambda^{1/2} = v_f / v_m \qquad (4)$$

where λ, L, A, F, ρ, and v are the ratio of the length scale, length, area, force, water density, and towing speed, respectively.

Trawl Design

The bottom trawl design used in this study was a 4-panel, 2-bridle, high opening AngCos 3325 small mesh shrimp trawl net manufactured by Isfell EHF in Iceland. The headline length was 60.4 m, and the fishing line length was 71.4 m. Floatation on the headline was provided by 232 trawl floats (200 Isfell titanium 200 mm Ø 2.90 kg of lift and 32 Atlantic floats 242 mm Ø 4.28 kg of lift). Additional floats were added along the selvedges (*n* = 25 titanium 200 mm Ø) and fishing line (*n* = 160 titanium 200 mm Ø). Mesh sizes ranged from 200 to 50 mm, and towing speed during fishing operations is 1.29 m s^{-1} (2.5 knots).

Traditional Footgear

Two types of model footgears were scaled

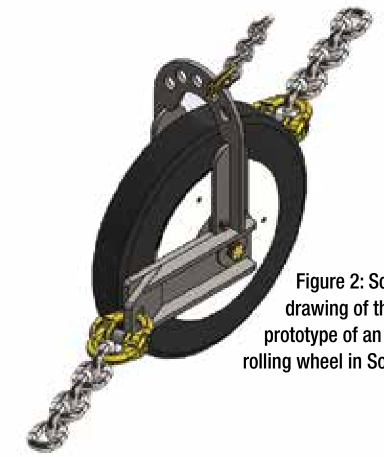

Figure 2: Schematic drawing of the full-scale prototype of an aligned-rolling wheel in SolidWorks.

and constructed for flume tank testing. The traditional footgear was typical of that used by commercial fishing vessels in Eastern Canada. In full-scale terms, it consisted of five rolling footgear sections; a 4.4 m bosom section with 12 rubber discs, a port, and starboard 4.0 m first bunt wing section with seven rubber discs, and a second port and starboard bunt wing section with five rubber discs (Figure 1). Each section contained rubbers, spacers, weights, and lancasters distributed along its length. Sections were connected by swivels, and 0.61 m diameter steel bobbins were placed in between sections. The remainder of the footgear, i.e., port and starboard wing sections, were 22 m long, made of bare chain, and five steel bobbins of 0.61 m diameter. Dan Leno assemblies with a 0.61 m diameter bobbin were used after the second bunt wing and wing sections. The bosom section had 22 mm chain, while the remainder of the footgear had 19 mm chain. Toggle chains were 72 cm, complying with local fishing regulations. Rubber discs were 0.61 m in diameter. In total, there were 36 rubber discs and 18 steel bobbins in contact with the seafloor. Full-scale weight in seawater was 2.11 t.

Aligned-rolling Footgear

The aligned-rolling footgear consists of the same bosom section as the traditional footgear; however, the first and second bunt wing sections were replaced by a bare chain and four aligned-rolling rubber wheels (Figure 2). Wing sections were replaced by a bare chain and five aligned-rolling rubber wheels (Figure 1). The aligned-rolling rubber wheels were 0.61 m in diameter. Port and starboard wing Dan Leno assemblies with bobbin and first bobbin were also present in the aligned-rolling footgear configuration. The bosom section had 22 mm chain, while the remainder of the footgear had 19 mm chain. Toggle chains were 72 cm long to comply with fishing regulations. Rubber discs were 0.61 m in diameter. In total, the aligned-rolling footgear consisted of 12 rubber discs, 18 aligned wheels, and four steel bobbins in contact with the seafloor. Full-scale weight in seawater was 2.03 t.

Alignment of the wheels with the towing direction is critically important for an aligned footgear to work effectively [He and Balzano, 2010]. This was achieved in the flume tank by measuring the distance between the bobbins along the traditional footgear at a simulated towing speed of 1.29 m s^{-1} (2.5 knots), and 65 m door spread. Angles of towing direction with respect to the footgear chain direction were then calculated for an effective design of the aligned wheel components in the bunt wing and wing sections.

Simulated Seafloor Experiment

Three aluminum plates of 1.22 m by 2.44 m (12.2 and 24.4 m full-scale) were used to simulate smooth, semi-rough, and rough seabed conditions for the flume tank testing

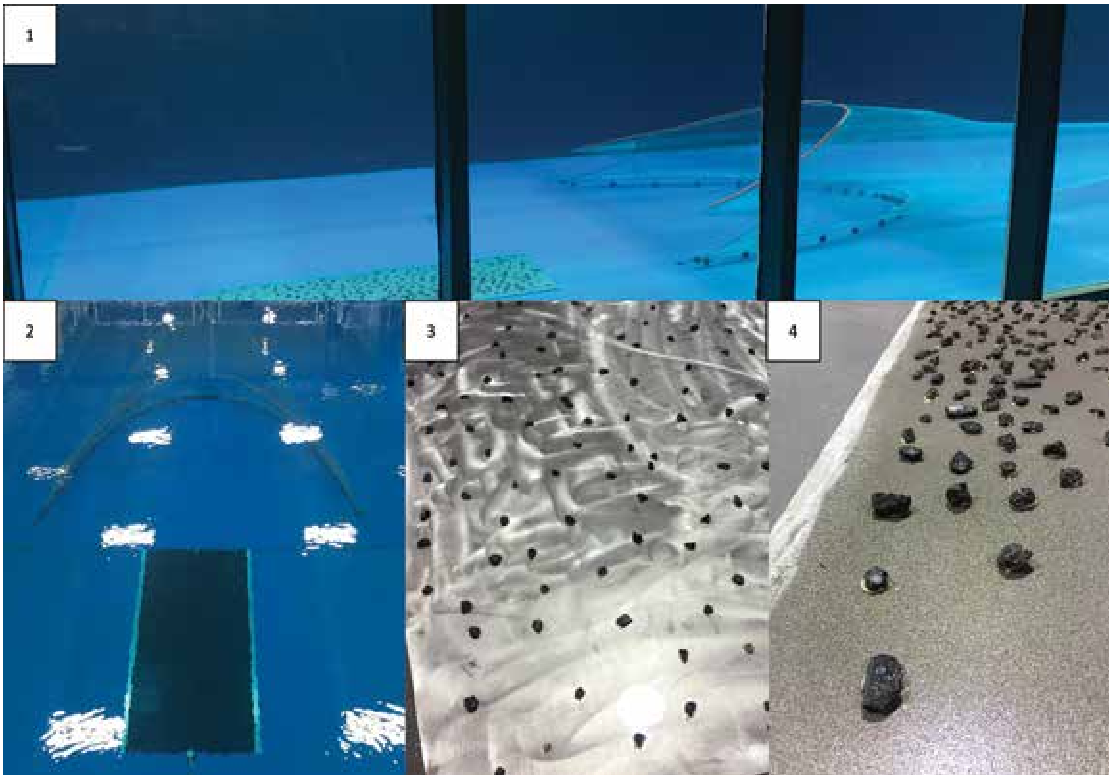

Figure 3: (1) Bottom trawl with aligned-rolling footgear during flume tank testing with the rough plate in the wing section. (2) Bottom trawl with aligned-rolling footgear during flume tank testing with the smooth plate in the bosom section. (3) Close-up view of the semi-rough and (4) rough seabed conditions.

of the traditional and experimental footgear (Figure 3). The smooth plate had a coat of paint for extra smoothness. The semi-rough plate had 139 rocks glued with PL Premium™ construction adhesive, with a mean height of 0.010 m (0.10 m full-scale). The rough plate had 353 rocks glued, with a mean height of 0.014 m (0.14 m full-scale). Rocks were selected by size for each plate and randomly distributed on the surface (Figure 3).

The experiment began by deploying the model bottom trawl in the flume tank with gentle water flow (i.e., 0.5 m s^{-1} full-scale). The port and starboard warps were attached to a load cell and lowered to a height of 0.19 m off the seabed using the towing masts (see [Winger et al., 2006]). The width of the towing masts was set up to simulate a 65 m full-scale door spread, producing a lower wing-end spread of 37.13 m. Once the trawl was in place, the water flow was stopped, and an aluminum plate (smooth, semi-rough, or rough seabed condition) was lowered and placed on top of the flume tank belt, aligned with the centre of the bosom section or with the centre of the port wing section (Figure 3). Alignment of the plates with the specific footgear sections was achieved by marking the plates and using the flume tank belt lines as a reference. Once the plate was safely in place, the water flow was increased to a typical towing speed used by the fishing industry (1.29 m s^{-1} full-scale; 0.38 m s^{-1} model scale). The belt was then turned on, and the plate went under the bottom trawl. Once the plate was past the bottom trawl, the belt was stopped, the flow was reduced, the bottom trawl was lifted a few centimetres

Study	Components measured	Penetration depth (cm) in:		
		Mud	Sand	Gravel
[Smith et al., 2003]	Whole trawl (Ø not reported)	7-10	0.01-1.6	
[van Marlen et al., 2010]	40.6/45.7 cm Ø rockhopper discs	2.8		
	40.6 cm Ø bobbins	3.46		
[Freese et al., 1999]	0.6 cm Ø tires/0.45 cm Ø rockhopper discs			1-8
[Schwinghamer et al., 1996]	Rockhopper discs (Ø not reported)		4-5	

Table 1: Studies that measured seabed penetration depth (cm) at-sea of bottom trawls in mud, sand, and gravel.

from the belt, and the belt was reversed back to the original position. The above process was repeated five times for each of the two footgears, in two footgear sections, using three seabed conditions, for a total of 12 trials of five replicates.

Seabed Contact Calculation

The traditional and aligned-rolling footgear were drawn in AutoCAD 2019 using measurement data collected during flume tank testing at 1.29 m s^{-1}, 65 m door spread, with a flat moving belt. This provided information on the discs' alignment with respect to the towing direction. Following the same procedure as Nguyen et al. [2015a] and Winger et al. [2018], based on a selected penetration pathway of the discs and bobbins, the total contact width of the footgear components was calculated and divided by total footgear width to obtain the percentage of total seabed contact by the traditional and aligned-rolling footgears. Previous experiments have documented seabed penetration depth of bottom trawl nets in sand, mud, and gravel during sea trials, ranging from 0.01 to 10 cm (Table 1). As such, a range of modelled penetration depths were selected ranging from 1 to 13 cm with 3 cm intervals.

Warp Load Measurement

Two 45.4 kg load cells (Model-No. 31, Honeywell, USA) were used to record port and starboard warp load (kgf). Data acquisition hardware logged the data at a frequency of 50 Hz. Before starting the experiment, load cell data inputs were calibrated through a series of weight measurements (4, 6, 8, 14, and 20 kg). Bosom, bunt wing, and wing footgear sections were video recorded with time stamps during testing to correlate load data to when the plate was in contact with the footgear section. Raw loads (kgf) were imported to MS Excel. Port and starboard load measurements during footgear contact with the plate were extracted, added to obtain the total load (total load = port + starboard), converted to full-scale values (t), and averaged for each replicate measurement of footgear:section:seabed combination, following a similar approach as Tsukrov et al. [2011].

Model warp load (kgf) was converted to full-scale values (t), following force modelling law:

$$F_m = (F_f/\lambda^3)(\rho_m/\rho_f) \quad (5)$$

	Warp load (t) (SEM)					
	Bosom			Wing		
Footgear	Smooth	Semi rough	Rough	Smooth	Semi rough	Rough
Aligned	12.58 (0.07)	12.68 (0.08)	12.83 (0.01)	12.55 (0.02)	12.75 (0.02)	12.75 (0.05)
Traditional	12.84 (0.05)	13.36 (0.05)	13.57 (0.03)	12.92 (0.09)	13.00 (0.05)	13.05 (0.06)
Warp load reduction (t)	0.26	0.68	0.74	0.38	0.25	0.30
Warp load reduction (%)	2.02%	5.08%	5.45%	2.92%	1.95%	2.33%

Table 2: Observed mean warp loads (t) and standard error of the mean (SEM) for the traditional and aligned-rolling footgears in smooth, semi-rough, and rough seabed conditions in the bosom and wing section. Warp load reduction (t) from Tukey HSD and percentage reduction in warp load are shown.

where $\lambda = 10$, $\rho_m = 999.6\ kg\ m^{-3}$ and $\rho_f = 1026.0\ kg\ m^{-3}$, a force scale of 1:1026.41 was obtained.

Statistical Analysis

A three-way ANOVA was conducted to determine the effects of footgear section, seabed condition, and footgear type on the full-scale warp load using rstatix package [Kassambara, 2020] in statistical software R [R Core Team, 2020] with statistical significance considered at an alpha of 0.05. Pairwise comparisons of the mean warp loads were then conducted using a Tukey's honest significant difference test (Tukey HSD) using the stats package in statistical software R [R Core Team, 2020].

Three-way ANOVA assumptions were tested with residual analysis in R. Normality was assessed using Shapiro-Wilk's normality test, and Levene's test assessed homogeneity of variances. Residuals were normally distributed (p-value > 0.05) and there was homogeneity of variances (p-value > 0.05).

RESULTS

A total of 60 mean warp load values were obtained from the experiment; five for each footgear, section, and seabed combination. Observed mean warp loads ranged between 12.55 t for the aligned-rolling footgear with smooth seabed in the wing section up to 13.57 t for the traditional footgear with the rough seabed in the bosom section (Table 2). Observed mean warp load reductions from traditional to aligned-rolling footgear ranged between 1.95% to 5.54% for semi-rough condition in wing section and rough condition in bosom section, respectively (Table 2). Video recordings provided qualitative evidence that the aligned-rolling footgear wheels were rotating and in an upright position. Furthermore, they were able to go over the rocks of the plates, and there was no entanglement or damage to the footgear or bottom trawl during testing.

Depending on the footgear type and section, the plates contacted different components when passing under the model trawl. For the traditional footgear, in bosom location (i.e., plate aligned with the centre of the trawl), the plates made contact with 26 rubber discs and two bobbins, while in the port wing location (i.e., plate aligned with the centre of the port wing section), the plates contacted seven bobbins. For the aligned-rolling footgear, the bosom location of the plates produced contact with 12 rubber discs and six aligned-

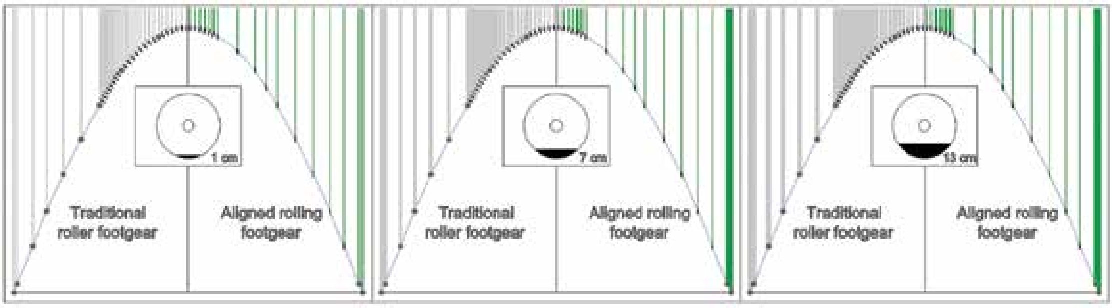

Figure 4: Seabed contact comparison for traditional and aligned-rolling footgear at three modelled pathway depths (1, 7, and 13 cm). Left drawing shows seabed contact for the traditional footgear (grey = 24.6%) and aligned-rolling footgear (green = 9.4%) at a modelled pathway depth of 1 cm. Middle drawing shows seabed contact for the traditional footgear (grey = 46.5%) and aligned-rolling footgear (green = 13.6%) at a modelled pathway depth of 7 cm. Right drawing shows seabed contact for the traditional footgear (grey = 53.5%) and aligned-rolling footgear (green = 15.3%) at a modelled pathway depth of 13 cm. Lateral view of rubber discs at the different penetration depths are shown for each drawing.

Modelled penetration depth (cm)	Seabed contact (m)		Seabed contact (%)		Contact reduction (%)
	Traditional	Aligned	Traditional	Aligned	
1	3.8	9.8	9.4%	24.6%	61.8%
4	4.9	16.0	12.3%	42.3%	69.4%
7	5.4	18.6	13.6%	46.5%	70.8%
10	5.7	19.8	14.4%	49.5%	71.0%
13	6.1	21.4	15.3%	53.5%	71.5%

Table 3: Seabed contact (m), seabed contact percentage (%) with respect to the total footgear width, and contact reduction (%) for the traditional and aligned-rolling footgear in modelled penetration depths of 1, 4, 7, 10, and 13 cm.

rolling wheels, while in the port wing location contacted two bobbins and five aligned-rolling wheels.

The seabed contact for the traditional footgear ranged between 24.6% and 53.5% of the total footgear width, depending on the depth penetration modelled (Figure 4, Table 3). In contrast, the seabed contact for the aligned-rolling footgear ranged between 9.4% and 15.3%. Thus, the reduction in seabed contact for the aligned-rolling footgear ranged between 61.8% and 71.5%, compared to the traditional footgear. AutoCAD drawings suggested that rubber disc angles with respect to the towing direction ranged between 3° to 25°, 32° to 51°, and 54° to 58° for the traditional footgear bosom, first bunt wing, and second bunt wing sections, respectively. The aligned-rolling footgear bosom section was identical to the traditional footgear bosom section; in consequence, the angles of the bosom rubber discs were the same (between 3° and 25°, with respect to the towing direction). The remainder of the rubber discs were aligned with the towing direction (0° angles).

Results from the ANOVA suggested a statistically significant three-way interaction between section, seabed condition, and

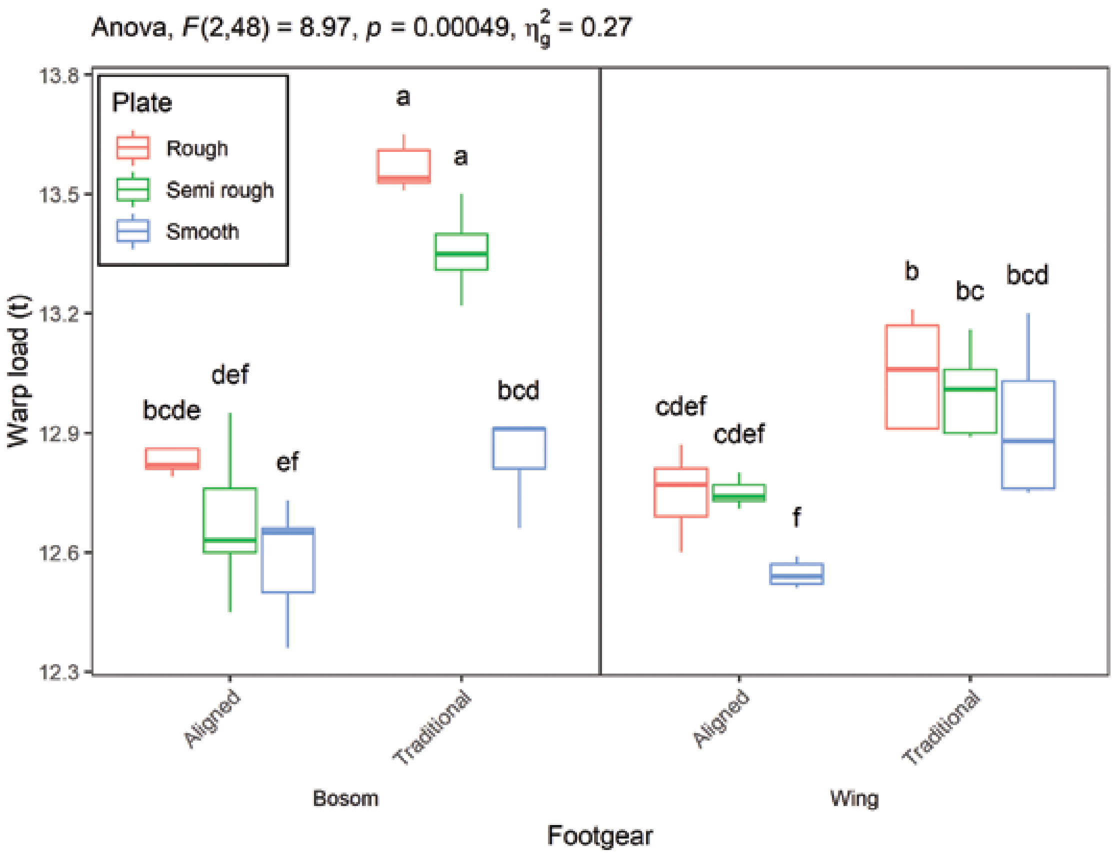

Figure 5: Boxplot of warp load for the aligned-rolling and traditional footgears with smooth, semi-rough, and rough seabed conditions in the bosom and wing footgear sections. Colours represent smooth, semi-rough, and rough seabed conditions. The horizontal line in the middle of the boxes represents the median load. The lower and upper limit of the boxes shows the first and third quartile, respectively. Lower and upper whiskers represent scores outside the interquartile range. Significant three-way interaction statistics are shown in the upper section. Tukey's HSD compact letter display on top of the boxes are showing which group means are significantly different from each other.

Effect	Degrees of freedom numerator	Degrees of freedom denominator	F statistic	*p*-value	Generalized eta squared
Section	1	48	20.364	<0.001	0.298
Seabed	2	48	39.973	<0.001	0.625
Footgear	1	48	203.946	<0.001	0.809
Section:Seabed	2	48	9.343	0.000374	0.28
Section:Footgear	1	48	16.433	0.000184	0.255
Seabed:Footgear	2	48	3.937	0.026105	0.141
Section:Seabed:Footgear	2	48	8.966	0.000491	0.272

Table 4: Three-way ANOVA table for warp load (t) of aligned-rolling and traditional footgears for smooth, semi-rough, and rough seabed conditions in the bosom and wing sections.

footgear ($F(2, 48) = 8.966$, p-value < 0.001) (Figure 5, Table 4). Tukey HSD post hoc test showed that the traditional footgear produced significantly higher mean warp loads for all seabed conditions in the bosom section, compared to the aligned-rolling footgear in that same section; warp load in traditional footgear was 0.26 t greater for the smooth plate ([0.003, 0.517] 95% C.I., p-value= 0.044), 0.68 t greater for the semi-rough plate ([0.42, 0.93] 95% C.I., p-value < 0.001), and 0.74 t greater for the rough plate ([0.48, 1.00] 95% C.I., p-value < 0.001) (Figure 5, Supplemental Table 1 located after "References"). With the plates in wing section, the mean warp load was significantly higher for traditional footgear in smooth plate (difference = 0.38 t [0.12, 0.63] 95% C.I., p-value < 0.001) and rough seabed (difference = 0.30 t [0.05, 0.56] 95% C.I., p-value = 0.008). For the semi-rough seabed, the mean warp load indicated a difference; however, the p-value was slightly over the alpha of 0.5 (difference = 0.25 t [-0.003, 0.51] 95% C.I., p-value = 0.055) (Figure 5, Supplemental Table 1 located after "References").

The traditional footgear experienced significantly higher warp loads in the bosom section for semi-rough and rough seabed conditions, compared to the same conditions for the wing section, with a statistically significant difference of 0.35 t [0.09, 0.61] 95% C.I. (p-value = 0.001) and 0.52 t [0.26, 0.78] 95% C.I. (p-value < 0.001), respectively. By comparison, the aligned-rolling footgear showed no significant difference in warp loads between bosom and wing sections, for either the semi-rough seabed (difference = 0.07 t [-0.19, 0.33] 95% C.I., p-value = 0.998) or the rough seabed (difference = -0.08 t [-0.34, 0.18] 95% C.I., p-value = 0.995) (Figure 5, Supplemental Table 1 located after "References").

DISCUSSION

This study documents a novel technique for comparing traditional and experimental footgears using engineering models and simulated seabed conditions in a flume tank. Footgears were qualitatively compared using direct observation and quantitatively assessed by measuring warp load during smooth, semi-rough, and rough seabed conditions. During qualitative observations, the dynamics of the traditional footgear model seemed to mimic very closely the dynamics of the full-scale traditional footgear observed at sea in Araya-Schmidt et al. [2021]; the bouncing of the footgear sections over the simulated seabed was realistic compared to the video collected on full-scale trawls at sea. The approach proved helpful for initial prototype validation before proceeding to expensive sea trials, supporting the fishing gear development cycle [Winger et al., 2006]. This same approach has been conducted for the development of novel trawl doors (e.g., [Sala et al., 2009]), netting (e.g., [Kebede and Winger, 2020]), and footgear (e.g., [Ball et al., 2003; Grimaldo et al., 2014]).

Results from our flume tank testing revealed that the aligned-rolling footgear substantially reduced the width of contact with the seabed compared to the traditional footgear. These results are encouraging, validating the simple concept that aligning footgear components with the towing direction can substantially reduce seabed contact width. Winger et al. [2018] found similar results when flume tank testing an aligned (non-rolling) footgear, which reduced the predicted contact width with the seabed by 60% at a modelled penetration depth of 5.08 cm. Similarly, Nguyen et al. [2015a] found reductions in contact width, from traditional to experimental footgear, of 84% and 91% for 9-drop chain and 5-drop chain footgears, respectively (modelled penetration depth = 5.08 cm). While the previous example produced greater reductions in contact width than this study, it is important to note that there is a trade-off between the width of contact and the risk to damage the trawl; an exposed fishing line near a rough seabed with large rocks will likely lead to more trawl damage. Therefore, it is fundamental to consider the seabed type when developing a new footgear.

Our results also revealed a significant reduction in warp load associated with the aligned-rolling footgear compared to the traditional footgear. We attribute the increased drag of the traditional footgear to the larger number of rubber discs and bobbins producing greater sliding friction forces against the seabed, especially rubber discs in the bunt wing sections that are not aligned with the towing direction. By comparison, the aligned-rolling footgear exhibited less drag due to fewer rubber discs, fewer bobbins, and the aligned-rolling wheels. The rolling nature of the wheels meant they experienced mainly rolling friction rather than sliding forces [Fridman, 1986]. The reduction in the cross-sectional area experienced by the aligned-rolling footgear presumably reduced hydrodynamic drag and could also have contributed to the overall reduction in warp tension [Fridman, 1986].

These results are consistent with Ball et al. [2003], in which a rollerball net (i.e., with aligned wheeled components) reduced towing force by 12% at-sea trials when compared with a traditional design. Previous flume tank experiments with flat moving belts have shown that drag is directly related to towing speed [Fiorentini et al., 2004; Queirolo et al., 2009], which is not our case, where water flow remained constant, and seabed condition was changed during the experiment. However, it would be interesting to understand the effect on drag of several towing speeds using this simulated seabed approach.

Warp loads observed in this study may differ from full-scale warp loads at-sea due to many factors, such as seabed type, wind, current, and swell [Fiorentini et al., 2004; Sala et al., 2009; Nguyen et al., 2015b]. However, with the addition of a simulated seabed in flume tank testing, model warp loads for the different seabed conditions provide an approximation of the expected differences in full-scale warp loads from smooth to rough conditions. Fiorentini et al. [2004] found less than 15% difference in warp load between model and full-scale trawl tests for the traditional trawl, but at the same time, large discrepancies for the experimental trawl were observed.

A key limitation of the reported study was the size of the plates. Ideally, the plates would have been large enough to cover the entire width of the trawl path, which would present a more realistic scenario and produce greater warp load differences between the footgears. Unfortunately, we needed to make trade-offs concerning safety, ease of deployment, and potential damage to the facility. We also recognize that the rocks in our study were permanently glued to the plates, whereas rocks on the seabed are commonly displaced by bottom trawls during full-scale fishing operations. For example, Freese et al. [1999] found that tire footgear, designed to bounce over the objects, displaced 19% of the boulders with a median size of 0.75 m in the trawl pathway. It would be of value to measure rock displacement by the aligned-rolling footgear. However, it is expected that traditional footgear would produce more rock and seabed material displacement when compared to aligned-rolling footgear. This was proven by Ball et al. [2003], where rollerball footgear reduced seabed debris material in the trawl net by 66% during sea trials. Experimental bottom fishing studies have shown that fishing gears that penetrate deeper in the sediment will increase depletion in abundance and produce a slower recovery to control conditions of the benthic community [Sciberras et al., 2018]. We hypothesize that full-scale aligned-rolling footgear, due to its aligned and rolling capacities, will reduce sliding forces and width of seabed contact, thus reducing penetration depth in the seabed during commercial operations.

An aligned rolling-footgear with reduced width of seabed contact, drag, and penetration depth would be beneficial for the fishing industry and ecosystem; it could potentially reduce seabed impact and fuel consumption, including CO_2 emissions. Not only fisheries managers are concerned about the consequences of fishing on the ecosystem, but also consumers prefer sustainable seafood certified by different organizations [Grieve et al., 2015; Kaiser et al., 2016]. An aligned-rolling footgear technology could aid in the certification of a fishery as sustainable, reducing ecosystem impacts, improving acceptance of seafood products, and increasing profit of the fishing activity.

CONCLUSIONS

This study documents a novel technique for comparing traditional and experimental footgears using engineering models and simulated seabed conditions in a flume tank. We show that an innovative aligned-rolling footgear performed well over smooth, semi-rough, and rough seabed conditions. The new footgear exhibited significantly lower warp loads compared to traditional footgear and is predicted to produce drastically lower contact with the seabed. Reduced drag was attributed to a reduction in contact points, alignment with towing direction, and rotation of the footgear components, replacing most of the sliding friction by rolling friction forces.

ACKNOWLEDGMENTS

This research was supported by the Nunavut Fisheries Association and the Ocean Frontier Institute (Module H) through the Canada First Research Excellence Fund. Special thanks to Craig Hollett for assisting with the flume tank testing. We thank Stephen King and Pete Brown for assisting with engineering, material choice for the full-scale aligned-rolling footgear, and preparation of Figure 2.

CRediT AUTHORSHIP CONTRIBUTION STATEMENT

Tomas Araya-Schmidt: Conceptualization, Methodology, Validation, Formal analysis, Investigation, Data curation, Writing

– original draft, Writing – review and editing, Visualization. **George Legge:** Conceptualization, Methodology, Validation, Investigation, Writing – review and editing. **Mark Santos:** Investigation, Writing – review and editing. **Shannon Bayse:** Writing – review and editing, Visualization. **Paul Winger:** Validation, Methodology, Resources, Writing – review and editing, Supervision, Project administration, Funding acquisition, Visualization.

REFERENCES

Amoroso, R.O.; Pitcher, C.R.; Rijnsdorp, A.D.; McConnaughey, R.A.; Parma, A.M.; Suuronen, P.; Eigaard, O.R.; Bastardie, F.; Hintzen, N.T.; Althaus, F.; Baird, S.J.; Black, J.; Buhl-Mortensen, L.; Campbell, A.B.; Catarino, R.; Collie, J.; Cowan, J.H.; Durholtz, D.; Engstrom, N.; Fairweather, T.P.; Fock, H.O.; Ford, R.; Gálvez, P.A.; Gerritsen, H.; Góngora, M.E.; González, J.A.; Hiddink, J.G.; Hughes, K.M.; Intelmann, S.S.; Jenkins, C.; Jonsson, P.; Kainge, P.; Kangas, M.; Kathena, J.N.; Kavadas, S.; Leslie, R.W.; Lewise, S.G.; Lundy, M.; Makin, D.; Martin, J.; Mazor, T.; Gonzalez-Mirelis, G.; Newman, S.J.; Papadopoulou, N.; Posen, P.E.; Rochester, W.; Russok, T.; Salal, A.; Semmens, J.M.; Silvan, C.; Tsoloso, A.; Vanelslander, B.; Wakefield, C.B.; Wood, B.A.; Hilborn, R.; Kaiser, M.J.; and Jennings, S. [2018]. *Bottom trawl fishing footprints on the world's continental shelves*. Proceedings of the National Academy of Sciences of the United States of America. U.S.A. 115, E10275–E10282. https://doi.org/10.1073/pnas.1802379115.

Araya-Schmidt, T.; Winger, P.D.; Santos, M.R.; Moret, K.; DeLouche, H.; Legge, G.; and Bayse, S.M. [2021]. *Investigating the performance of a roller footgear in the offshore shrimp fishery of Eastern Canada using underwater video*. Fisheries Research, Vol. 240, 105968. https://doi.org/10.1016/j.fishres.2021.105968.

Ball, B.; Linnane, A.; Munday, B.; Davies, R.; and McDonnell, J. [2003]. *The rollerball net: a new approach to environmentally friendly ottertrawl design*. Archive of Fishery and Marine Research, Vol. 50, pp. 193-203.

Brinkhof, J.; Larsen, R.B.; Herrmann, B.; and Grimaldo, E. [2017]. *Improving catch efficiency by changing ground gear design: case study of Northeast Atlantic cod (Gadus morhua) in the Barents Sea bottom trawl fishery*. Fisheries Research, Vol. 186, pp. 269-282. https://doi.org/10.1016/j.fishres.2016.10.008.

Collie, J.; Hiddink, J.G.; van Kooten, T.; Rijnsdorp, A.D.; Kaiser, M.J.; Jennings, S.; and Hilborn, R. [2017]. *Indirect effects of bottom fishing on the productivity of marine fish*. Fish and Fisheries, Vol. 18, pp. 619-637. https://doi.org/10.1111/faf.12193.

Collie, J.S.; Hermsen, J.M.; Valentine, P.C.; and Almeida, F.P. [2005]. *Effects of fishing on gravel habitats: assessment and recovery of benthic megafauna on Georges Bank*. American Fisheries Society Symposium, Vol. 41, pp. 325-343.

Depestele, J.; Degrendele, K.; Esmaeili, M.; Ivanovic, A.; Kröger, S.; O'Neill, F.G.; Parker, R.; Polet, H.; Roche, M.; Teal, L.R.; Vanelslander, B.; and Rijnsdorp, A.D. [2019]. *Comparison of mechanical disturbance in soft sediments due to* *tickler-chain SumWing trawl vs. Electro-fitted PulseWing trawl*. ICES Journal of Marine Science, Vol. 76, pp. 312-329. https://doi.org/10.1093/icesjms/fsy124.

Esmaeili, M. and Ivanović, A. [2014]. *Numerical modelling of bottom trawling ground gear element on the seabed*. Ocean Engineering, Vol. 91, pp. 316-328. https://doi.org/10.1016/j.oceaneng.2014.08.014.

Fiorentini, L.; Sala, A.; Hansen, K.; Cosimi, G.; and Palumbo, V. [2004]. *Comparison between model testing and full-scale trials of new trawl design for Italian bottom fisheries*. Fisheries Science, Vol. 70, pp. 349-359. https://doi.org/10.1111/j.1444-2906.2004.00813.x.

Freese, L.; Auster, P.J.; Heifetz, J.; and Wing, B.L. [1999]. *Effects of trawling on seafloor habitat and associated invertebrate taxa in the Gulf of Alaska*. Marine Ecology Progress Series, Vol. 182, pp. 119-126. https://doi.org/10.3354/meps182119.

Fridman, A.L. [1986]. *Calculations for fishing gear designs, FAO Fishing Manuals*. Fishing News Books Ltd., Surrey, 242p. https://doi.org/10.1016/0165-7836(88)90021-5.

Fridman, A.L. [1973]. *Theory and design of commercial fishing gear*. Israel Program for Scientific Translations, Jerusalem, 489p.

Gilkinson, K.; Paulin, M.; Hurley, S.; and Schwinghamer, P. [1998]. *Impacts of trawl door scouring on infaunal bivalves: results of a physical trawl door model/dense sand interaction*. Journal of Experimental Marine Biology and Ecology, Vol. 224, pp. 291-312. https://doi.org/10.1016/S0022-0981(97)00207-4.

Grieve, C.; Brady, D.C.; and Polet, H. [2015]. *Best practices for managing, measuring and mitigating the benthic impacts of fishing*. Marine Stewardship Council Science Series, Vol. 3, pp. 81-120.

Grimaldo, E.; Gjøsund, S.H.; Sistiaga, M.; and Larsen, R.B. [2014]. *Semi-circle plate spreading ground gear*. First Interim Report of the ICES-FAO Working Group on Fishing Technology and Fish Behaviour (WGFTFB), May 5-9, 2014. New Bedford, U.S.A.

He, P. [2007]. *Technical measures to reduce seabed impact of mobile fishing gears*. In: Kennelly, S.J. (Ed.), By-Catch Reduction in the World's Fisheries. Springer, Dordrecht, pp. 141-179. https://doi.org/10.1007/978-1-4020-6078-6_6.

He, P. and Balzano, V. [2010]. *Design and test of a wheeled groundgear to reduce seabed impact of trawling*. Final report submitted to the Northeast Consortium. University of Massachusetts Dartmouth - SMAST, New Bedford, MA. SMAST-CE-REP-2010-002.

He, P. and Winger, P.D. [2010]. *Effect of trawling on the seabed and mitigation measures to reduce impact*. In: He, P. (Ed.), Behavior of Marine Fishes: Capture Processes and Conservation Challenges. Blackwell Publishing, Hoboken, pp. 295-314. https://doi.org/10.1002/9780813810966.ch12.

Hiddink, J.G.; Jennings, S.; Kaiser, M.J.; Queirós, A.M.; Duplisea, D.E.; and Piet, G.J. [2006]. *Cumulative impacts of seabed trawl disturbance on benthic biomass, production, and species richness in different habitats*. Canadian Journal of Fisheries and Aquatic Science, Vol 63, pp. 721-736. https://doi.org/10.1139/f05-266.

Hiddink, J.G.; Jennings, S.; Sciberras, M.;

Szostek, C.L.; Hughes, K.M.; Ellis, N.; Rijnsdorp, A.D.; McConnaughey, R.A.; Mazor, T.; Hilborn, R.; Collie, J.S.; Pitcher, C.R.; Amoroso, R.O.; Parma, A.M.; Suuronen, P.; and Kaiser, M.J. [2017]. *Global analysis of depletion and recovery of seabed biota after bottom trawling disturbance*. Proceedings of the National Academy of Sciences of the United States of America. U.S.A. Vol. 114, pp. 8301-8306. https://doi.org/10.1073/pnas.1618858114.

Hu, F.; Matuda, K.; and Tokai, T. [2001]. *Effects of drag coefficient of netting for dynamic similarity on model testing of trawl nets*. Fisheries Science, Vol. 67, No. 1, pp. 84-89. https://doi.org/10.1046/j.1444-2906.2001.00203.x.

Ivanovic, A.; Neilson, R.D.; and Chima-okereke, C. [2009]. *Modelling of the interaction between trawl gear components and the seabed – overview*. DEMAT, pp. 21-31.

Ivanović, A.; Neilson, R.D.; and O'Neill, F.G. [2011]. *Modelling the physical impact of trawl components on the seabed and comparison with sea trials*. Ocean Engineering, Vol. 38, pp. 925-933. https://doi.org/10.1016/j.oceaneng.2010.09.011.

Ivanović, A. and O'Neill, F.G. [2015]. *Towing cylindrical fishing gear components on cohesive soils*. Computers and Geotechniques, Vol. 65, pp. 212-219. https://doi.org/10.1016/j.compgeo.2014.12.003.

Ivanović, A.; Zhu, J.; Neilson, R.; and O'Neill, F.G. [2008]. *Physical impact of a roller clump on the seabed*. Proceedings of the International Conference on Offshore Mechanics and Arctic Engineering – OMAE. pp. 723-727. https:// doi.org/10.1115/OMAE2008-57978.

Jennings, S.; Pinnegar, J.K.; Polunin, N.V.C.; and Warr, K.J. [2001]. *Impacts of trawling disturbance on the trophic structure of benthic invertebrate communities*. Marine Ecology Progress Series, Vol. 213, pp. 127-142. https://doi.org/10.3354/meps213127.

Johnson, A.F.; Gorelli, G.; Rees, S.; Hiddink, J.G.; and Hinz, H. [2015]. *Effects of bottom trawling on fish foraging and feeding*. Proceedings of the Royal Society B: Biological Sciences, Vol. 282, no. 1799. https://doi.org/10.1098/rspb.2014.2336.

Kaiser, M.J.; Hilborn, R.; Jennings, S.; Amaroso, R.; Andersen, M.; Balliet, K.; Barratt, E.; Bergstad, O.A.; Bishop, S.; Bostrom, J.L.; Boyd, C.; Bruce, E.A.; Burden, M.; Carey, C.; Clermont, J.; Collie, J.S.; Delahunty, A.; Dixon, J.; Eayrs, S.; Edwards, N.; Fujita, R.; Gauvin, J.; Gleason, M.; Harris, B.; He, P.; Hiddink, J.G.; Hughes, K.M.; Inostroza, M.; Kenny, A.; Kritzer, J.; Kuntzsch, V.; Lasta, M.; Lopez, I.; Loveridge, C.; Lynch, D.; Masters, J.; Mazor, T.; McConnaughey, R.A.; Moenne, M.; Francis; Nimick, A.M.; Olsen, A.; Parker, D.; Parma, A.; Penney, C.; Pierce, D.; Pitcher, R.; Pol, M.; Richardson, E.; Rijnsdorp, A.D.; Rilatt, S.; Rodmell, D.P.; Rose, C.; Sethi, S.A.; Short, K.; Suuronen, P.; Taylor, E.; Wallace, S.; Webb, L.; Wickham, E.; Wilding, S.R.; Wilson, A.; Winger, P.; and Sutherland, W.J. [2016.] *Prioritization of knowledge-needs to achieve best practices for bottom trawling in relation to seabed habitats*. Fish and Fisheries, Vol. 17, pp. 637-663. https://doi.org/10.1111/faf.12134.

Kassambara, A. [2020]. *Pipe-friendly framework for basic statistical tests – rstatix*. Retrieved from: https://rpkgs.

datanovia.com/rstatix.
Kebede, G.E. and Winger, P.D. [2020]. *A comparison of hydrodynamic forces in knotted and knotless netting, using both helix and conventional ropes for midwater trawls*. Aquaculture and Fisheries, Vol. 6, No. 1, pp. 96-105. https://doi.org/10.1016/j.aaf.2020.04.002.
Larsen, R.B.; Herrmann, B.; Brinkhof, J.; Grimaldo, E.; Sistiaga, M.; and Tatone, I. [2018]. *Catch efficiency of groundgears in a bottom trawl fishery: a case study of the Barents Sea haddock*. Marine and Coastal Fisheries, Vol. 10, No. 5, pp. 493-507. https://doi.org/10.1002/mcf2.10048.
Løkkeborg, S. [2005]. *Impacts of trawling and scallop dredging on benthic habitats and communities*. FAO Fisheries Technical Paper, No. 472, 58p.
Mayer, L.M.; Schick, D.F.; Findlay, R.H.; and Rice, D.L. [1991]. *Effects of commercial dragging on sedimentary organic matter*. Marine Environmental Research, Vol. 31, pp. 249-261. https://doi.org/10.1016/0141-1136(91)90015-Z.
Montgomerie, M. [2015]. *Basic fishing methods: a comprehensive guide to commercial fishing methods*. SEAFISH 106p.
Nguyen, T.X.; Walsh, P.; Winger, P.D.; Favaro, B.; Legge, G.; Moret, K.; and Grant, S.M. [2015a]. *Assessing the effectiveness of drop chain footgear at reducing bottom contact in the Newfoundland and Labrador shrimp trawl fishery*. Journal of Ocean Technology, Vol. 10, No. 2, pp. 60-77.
Nguyen, T.X.; Winger, P.D.; Orr, D.; Legge, G.; Delouche, H.; and Gardner, A. [2015b]. *Computer simulation and flume tank testing of scale engineering models: how well do these techniques predict full-scale at-sea performance of bottom trawls?* Fisheries Research, Vol. 161, pp. 217-225. https://doi.org/10.1016/j.fishres.2014.08.007.
O'Neill, F.G. and Ivanović, A. [2016]. *The physical impact of towed demersal fishing gears on soft sediments*. ICES Journal of Marine Science, Vol. 73, (Supplement 1): pp. 5-14. https://doi.org/10.1093/icesjms/fsv125.
O'Neill, F.G. and Summerbell, K.J. [2016]. *The hydrodynamic drag and the mobilisation of sediment into the water column of towed fishing gear components*. Journal of Marine Systems, Vol. 164, pp. 76-84. https://doi.org/10.1016/j.jmarsys.2016.08.008.
Paschen, M.; Richter, U.; and Köpnick, W. [2002]. *Trawl penetration in the seabed (TRAPESE)*, EC-final report, contract No. 96-006, University of Rostock.
Queirolo, D.; DeLouche, H.; and Hurtado, C. [2009]. *Comparison between dynamic simulation and physical model testing of new trawl design for Chilean crustacean fisheries*. Fisheries Research, Vol. 97, pp. 86-94. https://doi.org/10.1016/j.fishres.2009.01.005.
R Core Team. [2020]. *R: a language and environment for statistical computing*. R Foundation for Statistical Computing. Vienna, Austria.
Sala, A.; Farran, J. d. A.P.; Antonijuan, J.; and Lucchetti, A. [2009]. *Performance and impact on the seabed of an existing- and an experimental-otterboard: comparison between model testing and full-scale sea trials*. Fisheries Research, Vol.100, pp. 156-166. https://doi.org/10.1016/j.fishres.2009.07.004.
Schwinghamer, P.; Guigné, J.Y.; and Siu, W.C.

[1996]. *Quantifying the impact of trawling on benthic habitat structure using high resolution acoustics and chaos theory*. Canadian Journal of Fisheries and Aquatic Science, Vol. 53, pp. 288-296. https://doi.org/10.1139/f95-277.

Sciberras, M.; Hiddink, J.G.; Jennings, S.; Szostek, C.L.; Hughes, K.M.; Kneafsey, B.; Clarke, L.J.; Ellis, N.; Rijnsdorp, A.D.; McConnaughey, R.A.; Hilborn, R.; Collie, J.S.; Pitcher, C.R.; Amoroso, R.O.; Parma, A.M.; Suuronen, P.; and Kaiser, M.J. [2018]. *Response of benthic fauna to experimental bottom fishing: a global meta-analysis*. Fish and Fisheries, Vol. 19, pp. 698-715. https://doi.org/10.1111/faf.12283.

Sciberras, M.; Parker, R.; Powell, C.; Robertson, C.; Kröger, S.; Bolam, S.; and Geert Hiddink, J. [2016]. *Impacts of bottom fishing on the sediment infaunal community and biogeochemistry of cohesive and non-cohesive sediments*. Limnology and Oceanography, Vol. 61, pp. 2076-2089. https://doi.org/10.1002/lno.10354.

Smith, C.J.; Rumohr, H.; Karakassis, I.; and Papadopoulou, K.N. [2003]. *Analysing the impact of bottom trawls on sedimentary seabeds with sediment profile imagery*. Journal of Experimental Marine Biology and Ecology, Vol. 285-286, pp. 479-496. https://doi.org/10.1016/S0022-0981(02)00545-2.

Tauti, M. [1934]. *A relation between experiments on model and on full scale of fishing net*. Nippon Suisan Gakkaishi (Japanese edition), Vol. 3, No. 4, pp. 171-177. https://doi.org/10.2331/suisan.3.171.

Thierry, N.N.B.; Tang, H.; Achile, N.P.; Xu, L.; Hu, F.; and You, X. [2020]. *Comparative study on the full-scale prediction performance of four trawl nets used in the coastal bottom trawl fishery by flume tank experimental investigation*. Applied Ocean Research, Vol. 95, pp. 102022. https://doi.org/10.1016/j.apor.2019.102022.

Tillin, H.M.; Hiddink, J.G.; Jennings, S.; and Kaiser, M.J. [2006]. *Chronic bottom trawling alters the functional composition of benthic invertebrate communities on a sea-basin scale*. Marine Ecology Progress Series, Vol. 318, pp. 31-45. https://doi.org/10.3354/meps318031.

Tsukrov, I.; Drach, A.; Decew, J.; Robinson Swift, M.; and Celikkol, B. [2011]. *Characterization of geometry and normal drag coefficients of copper nets*. Ocean Engineering, Vol. 38, pp. 1979-1988. https://doi.org/10.1016/j.oceaneng.2011.09.019.

Valdemarsen, J.W. [2001]. *Technological trends in capture fisheries*. Ocean Coastal Management, Vol. 44, pp. 635-651. https://doi.org/10.1016/S0964-5691(01)00073-4.

Valdemarsen, J.W.; Jørgensen, T.; and Engås, A. [2007]. *Options to mitigate bottom habitat impact of dragged gears*, FAO. Fisheries Technical Paper, No. 506. 43p.

Van Denderen, P.D.; Bolam, S.G.; Hiddink, J.G.; Jennings, S.; Kenny, A.; Rijnsdorp, A.D.; and Van Kooten, T. [2015]. *Similar effects of bottom trawling and natural disturbance on composition and function of benthic communities across habitats*. Marine Ecology Progress Series, Vol. 541, pp. 31-43. https://doi.org/10.3354/meps11550.

van Marlen, B.; Piet, G.J.; Hoefnagel, E.; Taal, K.; Revill, A.S.; O'Neill, F.G.; Vincent, B.; Vold, A.; Rihan, D.; Polet, H.; Stouten, H.; Depestele, J.; Eigaard, O.R.; Dolmer, P.; Frandsen, R.P.; Zachariassen, K.; Innes, J.; Ivanovic, A.; Neilson, R.D.; Sala, A.; Lucchetti, A.; De Carlo, F.; Canduci, G.; and Robinson, L. [2010]. *Development of fishing gears with reduced effects on the environment (DEGREE)*. Final Publishable Activity Report-EU Contract SSP8-CT-2004-022576.

Watson, R.; Revenga, C.; and Kura, Y. [2006]. *Fishing gear associated with global marine catches. II. Trends in trawling and dredging*. Fisheries Research, Vol. 79, pp. 103-111. https://doi.org/10.1016/j.fishres.2006.01.013.

Winger, P.D.; DeLouche, H.; and Legge, G. [2006]. *Designing and testing new fishing gears: the value of a flume tank*. Marine Technology Society Journal, Vol. 40, pp. 44-49. https://doi.org/10.4031/002533206787353240.

Winger, P.D.; Munden, J.G.; Nguyen, T.X.; Grant, S.M.; and Legge, G. [2018]. *Comparative fishing to evaluate the viability of an aligned footgear designed to reduce seabed contact in northern shrimp bottom trawl fisheries*. Canadian Journal of Fisheries and Aquatic Science, Vol. 75, pp. 201-210. https://doi.org/10.1139/cjfas-2016-0461.

Zachariassen, K. [2004]. *Umhvørvisvinarligur trolgrunnur FRS smárit 04/4.* [In Faroese].

Supplemental Table 1: Tukey HSD comparisons with difference in warp load (t), lower and upper 95% Confidence Intervals (C.I.), and p-values. Significant p-values are in bold.

Comparison	Difference (t)	Lower 95% C.I.	Upper 95% C.I.	*p*-value
Wing:Control:Aligned-Bosom:Control:Aligned	-0.03	-0.29	0.22	1.000
Bosom:Semi rough:Aligned-Bosom:Control:Aligned	0.10	-0.16	0.35	0.974
Wing:Semi rough:Aligned-Bosom:Control:Aligned	0.17	-0.09	0.43	0.507
Bosom:Rough:Aligned-Bosom:Control:Aligned	0.25	-0.01	0.50	0.067
Wing:Rough:Aligned-Bosom:Control:Aligned	0.17	-0.09	0.42	0.525
Bosom:Control:Traditional-Bosom:Control:Aligned	0.26	0.00	0.52	**0.044**
Wing:Control:Traditional-Bosom:Control:Aligned	0.34	0.09	0.60	**0.002**
Bosom:Semi rough:Traditional-Bosom:Control:Aligned	0.78	0.52	1.03	**<0.001**
Wing:Semi rough:Traditional-Bosom:Control:Aligned	0.42	0.17	0.68	**<0.001**
Bosom:Rough:Traditional-Bosom:Control:Aligned	0.99	0.73	1.24	**<0.001**
Wing:Rough:Traditional-Bosom:Control:Aligned	0.47	0.22	0.73	**<0.001**
Bosom:Semi rough:Aligned-Wing:Control:Aligned	0.13	-0.12	0.39	0.827
Wing:Semi rough:Aligned-Wing:Control:Aligned	0.20	-0.05	0.46	0.243
Bosom:Rough:Aligned-Wing:Control:Aligned	0.28	0.03	0.54	**0.020**
Wing:Rough:Aligned-Wing:Control:Aligned	0.20	-0.05	0.46	0.256
Bosom:Control:Traditional-Wing:Control:Aligned	0.29	0.04	0.55	**0.013**
Wing:Control:Traditional-Wing:Control:Aligned	0.38	0.12	0.63	**<0.001**
Bosom:Semi rough:Traditional-Wing:Control:Aligned	0.81	0.55	1.07	**<0.001**
Wing:Semi rough:Traditional-Wing:Control:Aligned	0.46	0.20	0.71	**<0.001**
Bosom:Rough:Traditional-Wing:Control:Aligned	1.02	0.77	1.28	**<0.001**
Wing:Rough:Traditional-Wing:Control:Aligned	0.51	0.25	0.76	**<0.001**
Wing:Semi rough:Aligned-Bosom:Semi rough:Aligned	0.07	-0.18	0.33	0.998
Bosom:Rough:Aligned-Bosom:Semi rough:Aligned	0.15	-0.11	0.41	0.686
Wing:Rough:Aligned-Bosom:Semi rough:Aligned	0.07	-0.19	0.33	0.998
Bosom:Control:Traditional-Bosom:Semi rough:Aligned	0.16	-0.09	0.42	0.579
Wing:Control:Traditional-Bosom:Semi rough:Aligned	0.25	-0.01	0.50	0.071
Bosom:Semi rough:Traditional-Bosom:Semi rough:Aligned	0.68	0.42	0.93	**<0.001**
Wing:Semi rough:Traditional-Bosom:Semi rough:Aligned	0.33	0.07	0.58	**0.004**
Bosom:Rough:Traditional-Bosom:Semi rough:Aligned	0.89	0.63	1.15	**<0.001**
Wing:Rough:Traditional-Bosom:Semi rough:Aligned	0.37	0.12	0.63	**<0.001**
Bosom:Rough:Aligned-Wing:Semi rough:Aligned	0.08	-0.18	0.33	0.996
Wing:Rough:Aligned-Wing:Semi rough:Aligned	0.00	-0.26	0.25	1.000
Bosom:Control:Traditional-Wing:Semi rough:Aligned	0.09	-0.17	0.35	0.986
Wing:Control:Traditional-Wing:Semi rough:Aligned	0.17	-0.08	0.43	0.472
Bosom:Semi rough:Traditional-Wing:Semi rough:Aligned	0.61	0.35	0.86	**<0.001**
Wing:Semi rough:Traditional-Wing:Semi rough:Aligned	0.25	-0.003	0.51	0.055
Bosom:Rough:Traditional-Wing:Semi rough:Aligned	0.82	0.56	1.07	**<0.001**
Wing:Rough:Traditional-Wing:Semi rough:Aligned	0.30	0.05	0.56	**0.009**
Wing:Rough:Aligned-Bosom:Rough:Aligned	-0.08	-0.34	0.18	0.995
Bosom:Control:Traditional-Bosom:Rough:Aligned	0.01	-0.24	0.27	1.000
Wing:Control:Traditional-Bosom:Rough:Aligned	0.10	-0.16	0.35	0.977
Bosom:Semi rough:Traditional-Bosom:Rough:Aligned	0.53	0.27	0.78	**<0.001**
Wing:Semi rough:Traditional-Bosom:Rough:Aligned	0.18	-0.08	0.43	0.454
Bosom:Rough:Traditional-Bosom:Rough:Aligned	0.74	0.48	1.00	**<0.001**
Wing:Rough:Traditional-Bosom:Rough:Aligned	0.22	-0.03	0.48	0.141
Bosom:Control:Traditional-Wing:Rough:Aligned	0.09	-0.16	0.35	0.984

Wing:Control:Traditional-Wing:Rough:Aligned	0.18	-0.08	0.43	0.454
Bosom:Semi rough:Traditional-Wing:Rough:Aligned	0.61	0.35	0.86	**<0.001**
Wing:Semi rough:Traditional-Wing:Rough:Aligned	0.26	0.00	0.51	0.051
Bosom:Rough:Traditional-Wing:Rough:Aligned	0.82	0.56	1.08	**<0.001**
Wing:Rough:Traditional-Wing:Rough:Aligned	0.30	0.05	0.56	**0.009**
Wing:Control:Traditional-Bosom:Control:Traditional	0.08	-0.17	0.34	0.992
Bosom:Semi rough:Traditional-Bosom:Control:Traditional	0.52	0.26	0.77	**<0.001**
Wing:Semi rough:Traditional-Bosom:Control:Traditional	0.16	-0.09	0.42	0.561
Bosom:Rough:Traditional-Bosom:Control:Traditional	0.73	0.47	0.98	**<0.001**
Wing:Rough:Traditional-Bosom:Control:Traditional	0.21	-0.04	0.47	0.197
Bosom:Semi rough:Traditional-Wing:Control:Traditional	0.43	0.18	0.69	**<0.001**
Wing:Semi rough:Traditional-Wing:Control:Traditional	0.08	-0.18	0.34	0.995
Bosom:Rough:Traditional-Wing:Control:Traditional	0.64	0.39	0.90	**<0.001**
Wing:Rough:Traditional-Wing:Control:Traditional	0.13	-0.13	0.38	0.853
Wing:Semi rough:Traditional-Bosom:Semi rough:Traditional	-0.35	-0.61	-0.10	**0.001**
Bosom:Rough:Traditional-Bosom:Semi rough:Traditional	0.21	-0.04	0.47	0.197
Wing:Rough:Traditional-Bosom:Semi rough:Traditional	-0.30	-0.56	-0.05	**0.009**
Bosom:Rough:Traditional-Wing:Semi rough:Traditional	0.56	0.31	0.82	**<0.001**
Wing:Rough:Traditional-Wing:Semi rough:Traditional	0.05	-0.21	0.30	1.000
Wing:Rough:Traditional-Bosom:Rough:Traditional	-0.52	-0.77	-0.26	**<0.001**